Measuring the formation energy barrier of skyrmions in zinc-substituted Cu_2OSeO_3

M. N. Wilson,[1] M. Crisanti,[2,3] C. Barker,[1] A. Štefančič,[3] J. S. White,[4] M. T. Birch,[1,5] G. Balakrishnan,[3] R. Cubitt,[2] and P. D. Hatton[1]

[1]*Department of Physics, Durham University, South Road, Durham DH1 3LE, United Kingdom*
[2]*Institut Laue-Langevin, Large Scale Structures Group, 71 avenue des Martyrs, CS 20156, 38042 Grenoble, Cedex 9, France*
[3]*Department of Physics, University of Warwick, Coventry CV4 7AL, United Kingdom*
[4]*Laboratory for Neutron Scattering and Imaging (LNS), Paul Scherrer Institut (PSI), CH-5232 Villigen PSI, Switzerland*
[5]*Diamond Light Source, Didcot OX11 0DE, United Kingdom*

(Received 1 February 2019; revised manuscript received 3 May 2019; published 22 May 2019)

We report small-angle neutron scattering (SANS) measurements of the skyrmion lattice in $(Cu_{0.976}Zn_{0.024})_2OSeO_3$ under the application of electric and magnetic fields. These measurements show an expansion of the skyrmion lattice stability region with electric field. Furthermore, using time-resolved SANS, we observe the slow formation of skyrmions after an electric or magnetic field is applied, which has not been observed in pristine Cu_2OSeO_3 crystals. The measured formation times are dramatically longer than the corresponding skyrmion annihilation times after the external field is removed, and increase exponentially from 100 s at 52.5 K to 10 000 s at 51.5 K. This thermally activated behavior indicates an energy barrier for skyrmion formation of 1.57(2) eV, the size of which demonstrates the huge cost for creating these complex chiral objects.

DOI: 10.1103/PhysRevB.99.174421

I. INTRODUCTION

Topological states of matter are the subject of extensive interest in condensed matter physics [1–4]. One such state, the skyrmion lattice, consists of topologically protected nanoscale magnetic solitons that form a hexagonal lattice [5]. Skyrmion lattices usually form only in a small region of magnetic field and temperature just below the magnetic-ordering temperature, and are typically stabilized by competition between the Dzyaloshinskii-Moriya interaction (DMI), symmetric exchange, and thermal fluctuations [4]. This state was first discovered in the noncentrosymmetric metallic compound MnSi that crystallizes in the $P2_13$ space group [6], and has since been found in isostructural materials such as FeGe [7], $Fe_{1-x}Co_xSi$ [8], and Cu_2OSeO_3 [9], in other noncentrosymmetric compounds [10–12], in thin films where skyrmions are stabilized by interfacial DMI [13–15] or by a combination of DMI, uniaxial anisotropy and geometric confinement [16–18], and in some centrosymmetric materials for which the state is thought to be stabilized by magnetic frustration [19,20].

Skyrmions have been proposed for spintronics applications as stable, nanoscale, storage elements [21,22]. One key requirement for this application is the ability to reliably perform a write operation by nucleating a skyrmion [23]. Cu_2OSeO_3 is seen as attractive from this perspective as it is an insulating magnetoelectric whose skyrmion phase stability can be enhanced by applying electric fields [24]. Furthermore, applying an electric field has been shown to nucleate skyrmions from either the competing conical state in bulk crystals [25] or the competing helical state in thin lamellae [26].

Another method for expanding the skyrmion region is to rapidly cool the system in a magnetic field to form metastable skyrmions. In Cu_2OSeO_3 [27] and other materials [28–30], this produces skyrmions that, at low temperature, exist for much longer than typical observation times. However, near the border of the equilibrium skyrmion pocket, metastable skyrmions are observed to annihilate with lifetimes shorter than are experimentally accessible (seconds) [29]. As a result of this short lifetime at higher temperatures, rapid cooling is required to stabilize a sizable metastable skyrmion population.

Recently, crystals of $(Cu_{1-x}Zn_x)_2OSeO_3$ ($x = 0$ to 0.024) have been grown and shown to host similar skyrmion phases to pristine Cu_2OSeO_3, but at temperatures shifted slightly lower as the Zn substitution level is increased [31]. Notably, the lifetime of metastable skyrmions in Zn-substituted crystals is dramatically enhanced compared to that seen in pristine Cu_2OSeO_3. This suggests a high sensitivity of the energetic balance between the conical and skyrmion phases to Zn substitution [32], in addition to the known sensitivity to applied electric fields [24,25]. It is therefore an interesting open question to determine the interplay of these two effects by studying how electric fields affect the skyrmion phase in $(Cu_{1-x}Zn_x)_2OSeO_3$ in comparison to how they affect skyrmions in pristine Cu_2OSeO_3.

In this paper, we use small-angle neutron scattering (SANS) to probe the skyrmion state in a crystal of $(Cu_{0.976}Zn_{0.024})_2OSeO_3$. We show that applying a positive electric field ($\vec{E} \parallel \vec{H}$) expands the temperature extent of the skyrmion pocket, while a negative electric field suppresses it, as is seen in pristine Cu_2OSeO_3 [24]. Furthermore, we find that skyrmions formed by the application of an electric field take a measurably long time to appear (100–10 000 s). The characteristic formation time is temperature dependent, allowing us to extract an energy barrier for the formation of skyrmions of 1.57(2) eV. This time-dependent behavior has not been observed in any other bulk skyrmion material. Our measurement of the energy barrier for skyrmion formation is an important advance in the understanding of skyrmion behavior.

II. EXPERIMENT DETAILS

A single crystal of $(Cu_{0.976}Zn_{0.024})_2OSeO_3$ ($T_C = 55.8$ K) was grown by chemical vapor transport (see Ref. [31] for details). From this crystal, a $1.08 \times 3 \times 3$ mm plate (thin axis $\parallel$ [111]) was cut and coated on both sides with silver paste to form conductive plates. With thin copper wires attached to the silver paste, the crystal was mounted on a sapphire plate in the Paul Scherrer Institut (PSI) high-voltage sample stick [33] and placed under vacuum. The evacuated sample stick was then inserted into a horizontal field cryomagnet on the PSI SANS-II instrument [34] to perform SANS measurements with 10 Å neutrons, under a magnetic and electric field $\vec{E} \parallel \vec{H} \parallel$ [111] crystal axis. SANS data analysis was performed using the $GRAS_{ANS}P$ software (v8.11b) from the Institut Laue-Langevin [35]. The ac susceptibility measurements were performed with $\vec{H} \parallel$ [111] using a Quantum Design MPMS-5S with an ac driving field of 3 Oe.

III. RESULTS AND DISCUSSION

Figure 1(a) shows a typical skyrmion SANS pattern taken at 54 K with $E = -2\,\mathrm{V}/\mu\mathrm{m}$ and $\mu_0 H = 26$ mT. The sixfold scattering pattern is characteristic of a skyrmion lattice with 61.30(1) nm spacing. Intensity in a ring between the main scattering spots arises from azimuthal rotational disorder in the skyrmion lattice, indicating a multidomain skyrmion state as has commonly been seen in Cu_2OSeO_3 [36–38] and is expected to be more prominent for samples with chemical substitutions [39]. To characterize the intensity of the skyrmion state (proportional to sample volume in the skyrmion state), we sum the intensity in the gray ring indicated on Fig. 1(a).

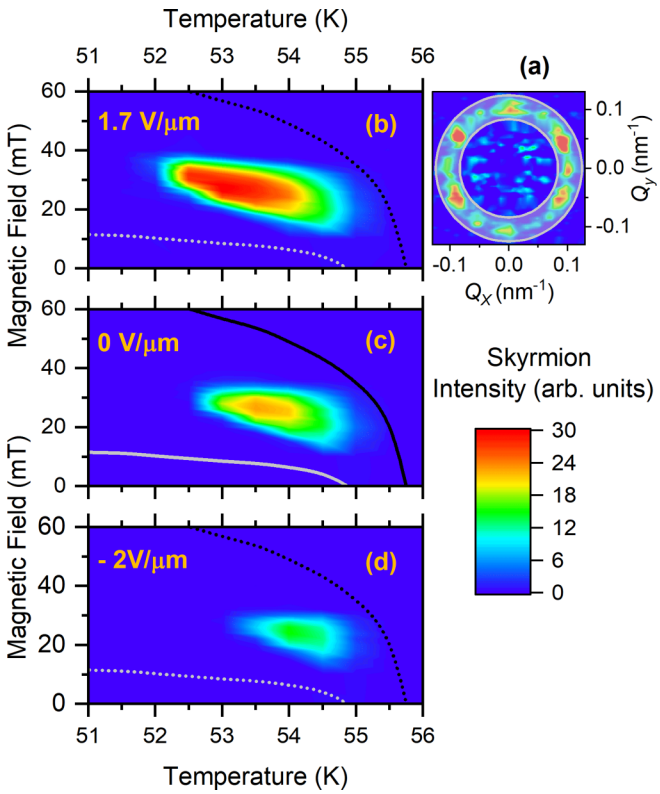

FIG. 1. (a) SANS pattern measured at 54 K with $E = -2\,\mathrm{V}/\mu\mathrm{m}$ and $\mu_0 H = 26$ mT. The gray ring shows the area that was summed on each pattern to characterize the skyrmion intensity. (b)–(d) Skyrmion phase diagrams of $(Cu_{0.976}Zn_{0.024})_2OSeO_3$ measured by SANS with increasing magnetic field sweeps after zero magnetic field cooling in applied electric fields of (b) $+1.7\,\mathrm{V}/\mu\mathrm{m}$, (c) 0, and (d) $-2\,\mathrm{V}/\mu\mathrm{m}$. The lines show the conical–field-polarized boundary (black) and the helical-conical boundary (gray) measured by ac susceptibility at $E = 0$.

Figures 1(b)–1(d) show the skyrmion intensity as a function of temperature and magnetic field for three different applied electric fields. The data show an enhancement and expansion of the skyrmion state by $0.5\,\mathrm{K}/(\mathrm{V}/\mu\mathrm{m})$ when a positive electric field is applied, and a corresponding suppression of the skyrmion state when a negative electric field is applied, consistent with that seen in pristine Cu_2OSeO_3 [24].

To further investigate the behavior of the skyrmions when an electric field is applied, we performed time-resolved SANS in the region $T \leqslant 52.6$ K, where the phase diagram indicates that skyrmions exist for an applied positive electric field but not for zero electric field. For these measurements we zero-field-cooled to the desired temperature, turned on the magnetic field, began ramping up the electric field, and commenced counting. After measuring the skyrmion lattice formation, we turned off the electric field, leaving the magnetic field on, and continued to count. A sample of these measurements is shown in Fig. 2 for $\mu_0 H = 34$ mT and $T = 52.25$ K. These data show that the skyrmion state takes significant time to form when the electric field is applied ($\tau_{\mathrm{form}} \approx 200$ s), but disappears much more rapidly when the electric field is removed ($\tau_{\mathrm{annihilate}} < 20$ s). Such behavior suggests a much larger energy barrier to form a skyrmion than to annihilate one. Further, Fig. 2 shows that the skyrmion intensity does not return to zero after the electric field is removed. This residual skyrmion intensity does not appear to arise from the metastable skyrmion state that has been previously seen when field cooling through the equilibrium state [27,32] as the intensity remains constant for 1000 s (1500–2500 s on Fig. 2), far longer than the expected 300 s lifetime of metastable skyrmions at this temperature [32]. Therefore, we suggest that the equilibrium skyrmion region at zero electric field extends below the region indicated by the phase diagram in Fig. 1(c), likely indicating that at low temperature the formation time becomes long compared to the measurement timescale. For the remainder of this paper we focus on characterizing the

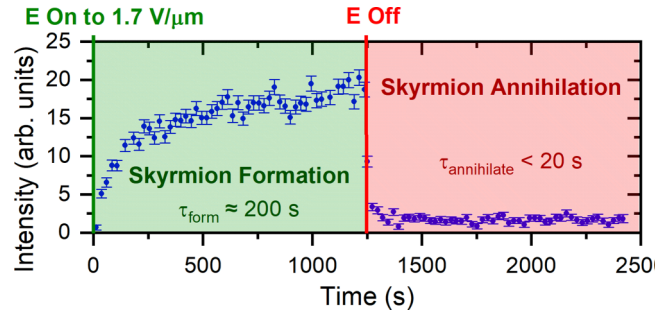

FIG. 2. Time dependence of skyrmion SANS intensity when applying and removing a $1.7\,\mathrm{V}/\mu\mathrm{m}$ electric field at 52.25 K and 34 mT.

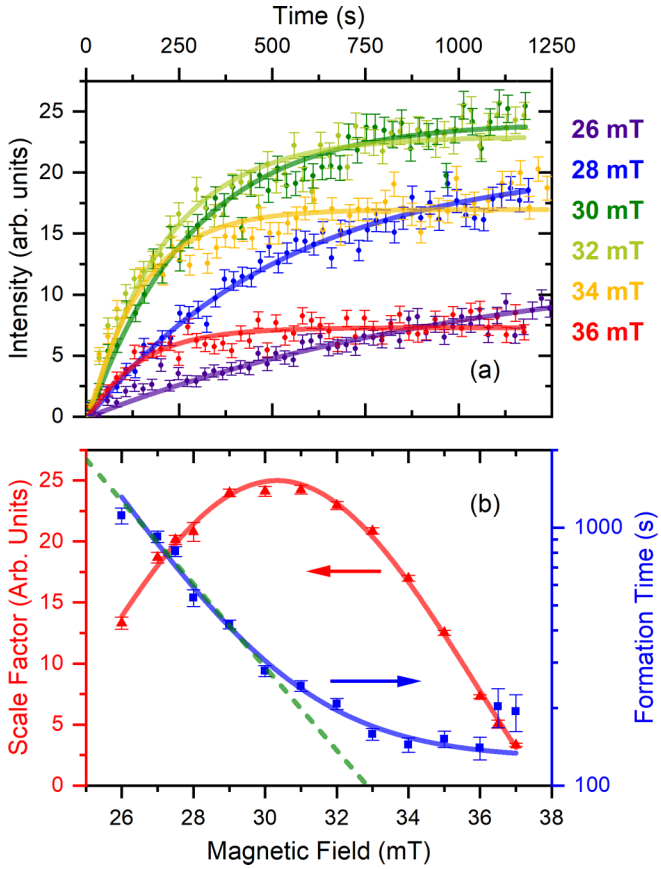

FIG. 3. Formation of skyrmions by applying an electric field of $1.7\,\mathrm{V}/\mu\mathrm{m}$ at 52.25 K in varied magnetic fields. (a) Skyrmion SANS intensity as a function of time. (b) Fit formation time (blue squares plotted on a log scale) and intensity scale factor (red triangles) from Eq. (1). Solid lines in (b) show fits to a Gaussian peak and $\tau = Ae^{-\lambda\mu_0 H} + \tau_a$. The dashed line in (b) shows the pure exponential behavior ($\tau = A_1 e^{-\lambda_1 \mu_0 H}$) of the formation time below 30 mT.

formation time, as the annihilation times were too short to measure accurately.

To fit the skyrmion intensity S accounting for the ramping of the electric field (see Appendix), we use the equations

$$S = \begin{cases} A\left[1-(1+kt)^{\frac{-1}{ka}}\right], & t \leqslant t_0, \\ A\left[1-e^{\frac{-t}{\tau}}\dfrac{(1+kt_0)^{\frac{-1}{ka}}}{e^{\frac{-t_0}{\tau}}}\right], & t > t_0. \end{cases} \quad (1)$$

Here, A is a scale factor for the skyrmion intensity, $\tau = a(1 + kt_0)$ is the reported formation time, a is allowed to vary with temperature and magnetic field, k accounts for the electric field ramp rate ($k = -0.0133\ \mathrm{s}^{-1}$ for Fig. 3 and $-0.008\ \mathrm{s}^{-1}$ for Fig. 4), and t_0 is the time when the electric field finished ramping.

Using this fitting function, we characterized the skyrmion formation time across the magnetic-field–temperature phase diagram. Figure 3(a) shows measurements of skyrmion formation after applying an electric field of $1.7\,\mathrm{V}/\mu\mathrm{m}$ at 52.25 K, as a function of magnetic field. Between each measurement, we reset the magnetic state by setting both the magnetic and electric field to zero at 52.25 K. Figure 3(b) shows

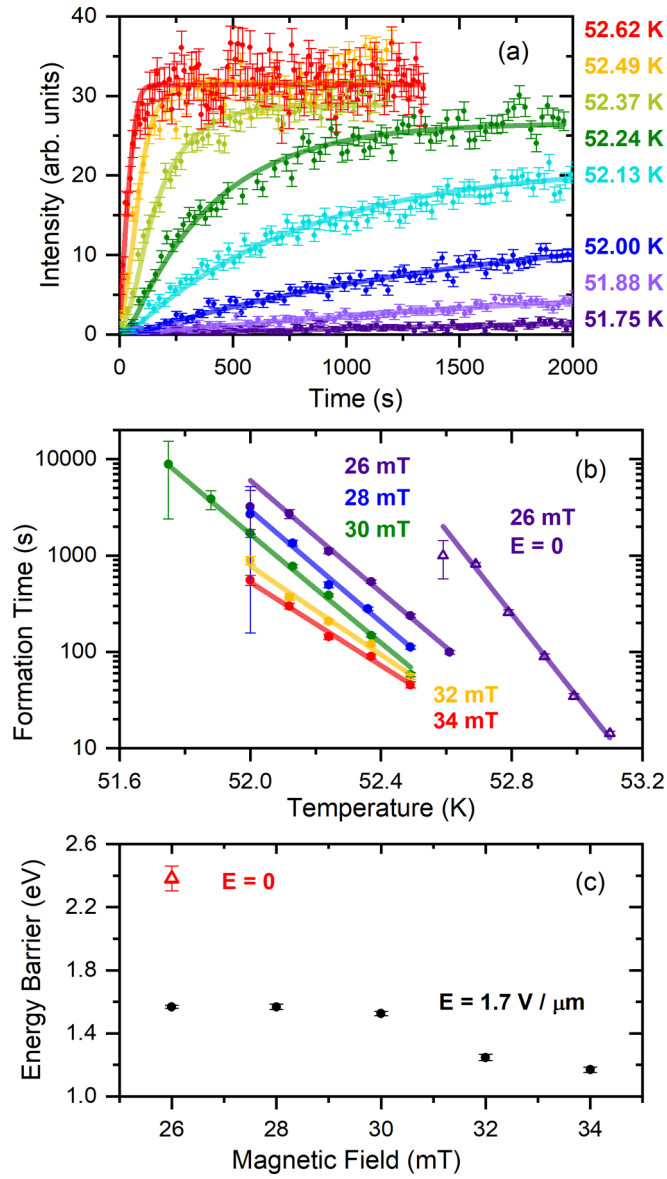

FIG. 4. (a) Skyrmion SANS intensity as a function of time after switching on $E = 1.7\,\mathrm{V}/\mu\mathrm{m}$ at $\mu_0 H = 30\,\mathrm{mT}$ for temperatures between 51.75 and 52.62 K. (b) Formation times as a function of temperature. Circles show formation times after switching on $E = 1.7\,\mathrm{V}/\mu\mathrm{m}$ in various magnetic fields. Purple triangles show the formation time after switching on $\mu_0 H = 26\,\mathrm{mT}$ in zero applied electric field. Lines show fits to an Arrhenius law. (c) Energy barriers from fits in panel (b) for $E = 1.7\,\mathrm{V}/\mu\mathrm{m}$ (black circles) and $E = 0$ (red triangle).

the fitted scale factor and formation time as a function of field. The scale factor is well described by a Gaussian curve centered at 30.3(1) mT, which may partially be caused by magnetic field inhomogeneity arising from demagnetization field effects [40]. The formation time is asymmetric across the skyrmion pocket, at first rapidly decreasing, then asymptoting to $\tau_a = 130(10)$ s at high field, phenomenologically fitting to $\tau = Ae^{-\lambda\mu_0 H} + \tau_a$, where $\lambda = 0.48(5)\ \mathrm{mT}^{-1}$.

Figure 4(a) shows skyrmion formation after applying a $1.7\,\mathrm{V}/\mu\mathrm{m}$ electric field for various temperatures in an applied

magnetic field of 30 mT. These data indicate an increasing formation time for decreasing temperature, characteristic of thermal activation over an energy barrier. In Fig. 4(b), we show fits of the formation times to an Arrhenius law, $\tau = \tau_0 e^{\frac{E}{k_B T}}$, to extract the energy barrier E, where τ_0 is a scale factor, and T is temperature. Fits of data obtained at five different applied magnetic fields yield energy barriers between 1.57(2) eV (26 mT) and 1.17(2) eV (34 mT), as shown by the black circles in Fig. 4. The energy barrier is nearly constant up to 30 mT, decreasing thereafter for higher magnetic fields. This change in the energy barrier is consistent with the magnetic field values where the formation time in Fig. 3(b) deviates from pure exponential behavior, suggesting that the reason for the apparent saturation of the formation time at high fields is a change in the skyrmion formation energy barrier. Some of the variation in the formation time with magnetic field may also arise from entropic effects changing the number of available pathways over the energy barrier between the conical and skyrmion states, as has been seen for the decay of metastable skyrmions in $Fe_{0.5}Co_{0.5}Si$ [41].

To determine whether this skyrmion formation behavior is solely an electric field effect or inherent to the skyrmion state, we performed time-dependent measurements when applying a magnetic field in constant electric field to compare with the process of turning on an electric field in a constant magnetic field. As our cryomagnet changed the magnetic field very rapidly, $S = A(1 - e^{-\frac{t}{\tau}})$ fits this data with no correction required for ramping time. These data are shown in Fig. 5(a) and demonstrate that the behavior is the same for both processes, yielding formation times that agree within their uncertainties. As an additional check, we compared measurements performed after switching a magnetic field on in zero electric field to measurements performed in a constant magnetic field after switching an electric field of $-1.7\,\mathrm{V}/\mu\mathrm{m}$ (which suppresses the skyrmion stability region) to zero (where skyrmions form). Shown in Fig. 5(b), these data again indicate no difference between the skyrmion formation behavior observed after the two processes. Figure 5 therefore shows that the factor affecting the formation time is the final magnetoelectric field state of the system, not the process by which it was brought there.

For comparison with the behavior observed in an applied electric field, we measured the temperature dependence of formation times when switching on a 26 mT magnetic field in zero electric field. Shown in Fig. 4(b), these formation times display a temperature dependence consistent with thermally activated behavior, similar to the data measured in a $1.7\,\mathrm{V}/\mu\mathrm{m}$ electric field. However, for the same magnetic field, the 2.38(8) eV energy barrier measured with zero electric field [red triangle in Fig. 4(c)] is substantially larger than the 1.57(2) eV barrier measured with an applied electric field, demonstrating that the electric field suppresses the energy barrier between the conical and skyrmion states.

Energy barriers for skyrmion annihilation have previously been measured in systems such as FeGe (0.19 eV) [42], $Fe_{0.5}Co_{0.5}Si$ (0–0.2 eV) [41], and Cu_2OSeO_3 (0.4 eV) [32], and are substantially smaller than our measured energy barriers for skyrmion formation. This is consistent with Fig. 2 showing that skyrmion annihilation is faster than skyrmion formation, and with theoretical predictions of smaller energy barriers for skyrmion annihilation than for skyrmion formation [43].

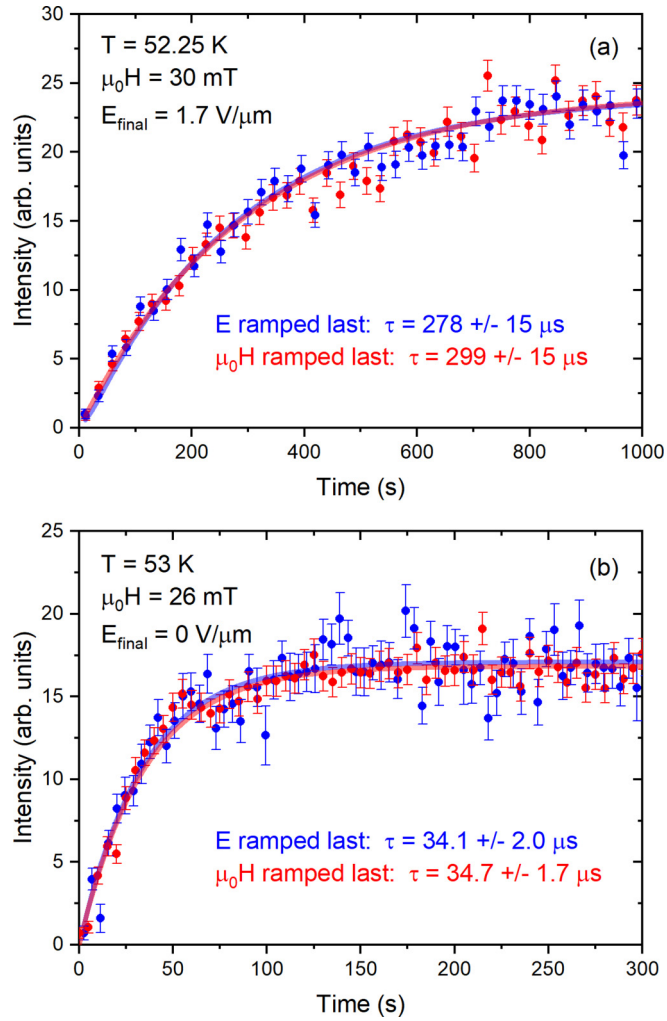

FIG. 5. (a) Skyrmion SANS intensity as a function of time measured at $E = 1.7\,\mathrm{V}/\mu\mathrm{m}$, $\mu_0 H = 30\,\mathrm{mT}$, and $T = 52.25\,\mathrm{K}$. The red data show measurements when the electric field was turned on first, and then the magnetic field was turned on at $t = 0\,\mathrm{s}$. These are fitted to $S = A(1 - e^{-\frac{t}{\tau}})$. The blue data show measurements when the magnetic field was turned on first, and the electric field ramping begins at $t = 0\,\mathrm{s}$. These are fitted to Eq. (1). (b) Skyrmion SANS intensity as a function of time measured at $E = 0\,\mathrm{V}/\mu\mathrm{m}$, $\mu_0 H = 26\,\mathrm{mT}$, and $T = 53\,\mathrm{K}$. The red data show measurements where the magnetic field was turned on at time = 0 in zero electric field. The blue data show measurements in a constant magnetic field where the electric field was changed from $-1.7\,\mathrm{V}/\mu\mathrm{m}$ to 0 at $t = 0\,\mathrm{s}$. Both data sets were fitted to $S = A(1 - e^{-\frac{t}{\tau}})$ as the magnetic field changes quickly and the electric field changes quickly when set to zero.

Formation times long enough to measure with SANS have not previously been seen in similar electric-field-switching experiments on crystals of pristine Cu_2OSeO_3 [25], which suggests that the formation times in our Zn-substituted samples are dramatically longer than those in the pristine material. Previous measurements of Zn-substituted crystals suggest that the lifetime of metastable skyrmions is substantially enhanced by entropic effects arising from the nonmagnetic substitution [32], which may also explain the long formation times.

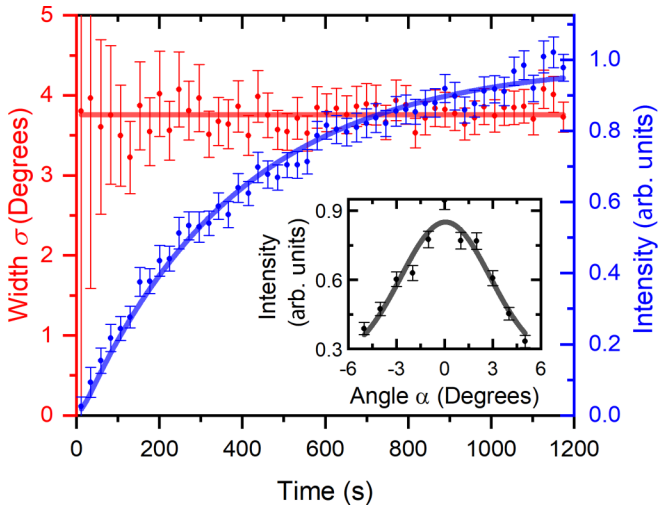

FIG. 6. Gaussian widths and intensities for SANS rocking curves measured during skyrmion formation at 52.25 K in a 30 mT magnetic field after applying a 1.7 V/μm electric field. The inset shows an example rocking curve constructed from data taken 20 minutes after applying the electric field.

However, it is also possible that Zn substitution does not change the skyrmion formation physics, and it is simply a reduction of the lower boundary of the skyrmion region from 55.5 K in pristine Cu_2OSeO_3 to 52.5 K in our Zn-substituted sample [31] that lengthens the formation time. Extrapolating our zero-electric-field data to 55.5 K, we would expect a formation time of $2.1^{+4.6}_{-0.9}$ ns, which is too short to observe with SANS.

It has previously been proposed that skyrmions form [44] and are annihilated [28,45] by the nucleation of Bloch points to create skyrmion strings, which then grow by propagation of the Bloch points. SANS measurements are sensitive to the average length of skyrmion strings by the width of rocking curves obtained by measuring the SANS intensity while rotating the sample and field together around the incoming beam direction (angle α). If the skyrmion strings are short, the rocking-curve width will be large, and as the strings grow the width is expected to decrease.

To study this process, we performed a series of skyrmion formation measurements at different angles ($-5.5^\circ \leqslant \alpha \leqslant 5.5^\circ$), and stacked them to form effective rocking curves as a function of time, an example of which is shown in the inset of Fig. 6. The fit Gaussian widths of these curves are displayed in Fig. 6 and show no change as a function of time, while the intensity follows the same exponential behavior as the previously presented data collected at a single angle, yielding a consistent formation time (378 $\pm$ 14 s with rocking vs 386 $\pm$ 13 s at a single angle). This suggests that the skyrmion length does not slowly increase over time, but rather that skyrmions either initially appear as long strings, or that after nucleating small skyrmions, Bloch points propagate too fast to be observed with SANS. The increasing SANS intensity therefore most likely arises from an increasing number of skyrmions: Bloch point nucleation, rather than propagation, is the rate-limiting step for skyrmion formation. However, we note that our minimum rocking-curve width (corresponding to a skyrmion length of 150 nm) is inherently broadened by instrumental resolution and variations in skyrmion string alignment, reducing our sensitivity to long length scales.

As we infer that the SANS intensity increase corresponds to an increase in the number of skyrmions, our measured energy barrier is that required to nucleate a Bloch point and start formation of a skyrmion string. The energy barrier of 1.5–2.5 eV is enormous compared to the thermal energy of single spins ($400k_BT$ for $T = 52$ K), suggesting that Bloch points are extended multispin objects rather than single spins. In Cu_2OSeO_3 the base spin units are ferrimagnetic tetrahedra with three parallel and one antiparallel Cu^{2+} spins [46,47]. Considering the exchange interactions of $J = -3.6$ meV [48], the energy to flip a single Cu tetrahedron spin unit is $\approx$0.1 eV. This suggests that nucleating a Bloch point requires flipping $\approx$20 tetrahedra, corresponding to an initial size of a couple of nanometers, which is far smaller than the 61 nm skyrmion diameter. Our data therefore indicate that while Bloch points in chiral magnets are small relative to skyrmions, they are significantly larger than single spins.

IV. CONCLUSIONS

In conclusion, we have measured the temperature and magnetic field dependence of the skyrmion formation time in Zn-substituted Cu_2OSeO_3. This shows thermally activated behavior, with timescales ranging from 10 000 seconds at the lowest temperatures down to 100 seconds at the highest temperatures, giving a characteristic energy barrier for skyrmion formation of 1.57(2) eV. Combining our results for skyrmion formation with previous measurements of skyrmion annihilation allows a more complete picture of the energetics of skyrmions to be inferred, which will be highly important for future research towards skyrmionic devices.

Data presented in this paper are available at [49].

ACKNOWLEDGMENTS

We thank T. J. Hicken and T. Lancaster for useful discussions, as well as J. Debray and M. Bartkowiak for technical support. The neutron scattering experiments were performed at the Swiss Spallation Neutron Source (SINQ), Paul Scherrer Institut, Switzerland. This work was financially supported by the UK Skyrmion Project EPSRC Programme, Grant No. EP/N032128/1, and the Swiss National Science Foundation (SNF) Sinergia Network "NanoSkyrmionics" Grant No. CRSII5-171003. M.N.W. acknowledges the support of the Natural Sciences and Engineering Research Council of Canada (NSERC).

APPENDIX: ELECTRIC FIELD DEPENDENCE

For each of the measurements of the skyrmion formation time in an electric field, the ramping time of the electric field was non-negligible compared to the total measurement time. The electric field was ramped quickly from 0 to 0.9 V/μm (Fig. 3) or 0 to 1.4 V/μm (Fig. 4), and then at 0.009 (V/μm)/s up to the peak electric field of 1.7 V/μm, giving a ramp time (t_0) of 33.6 or 83.6 s. The formation time of skyrmions depends linearly on the electric field, as shown by Fig. 7, fitting to $\tau(E) = mE + b$. The ramp time for the

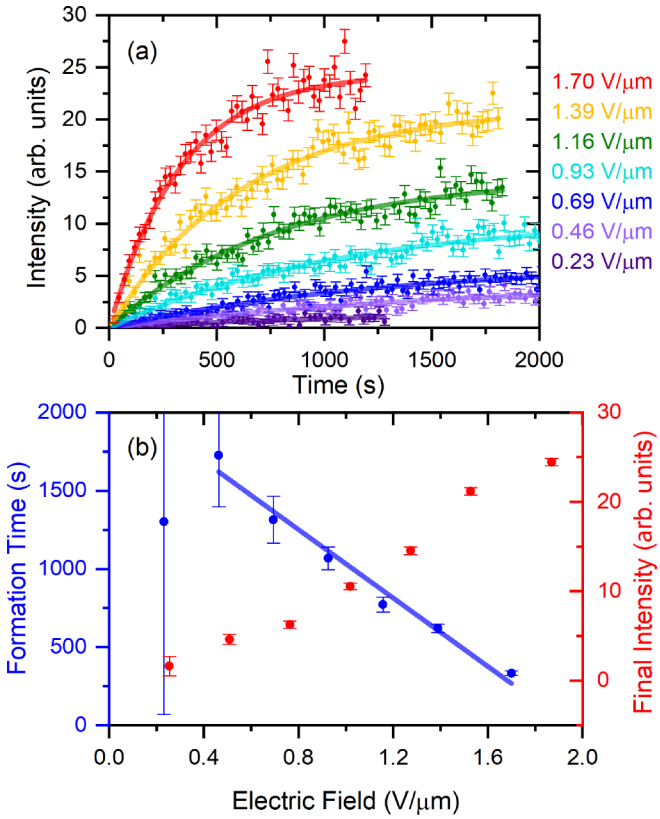

FIG. 7. Formation of skyrmions at 52.25 K in a magnetic field of 30 mT after applying various electric fields.

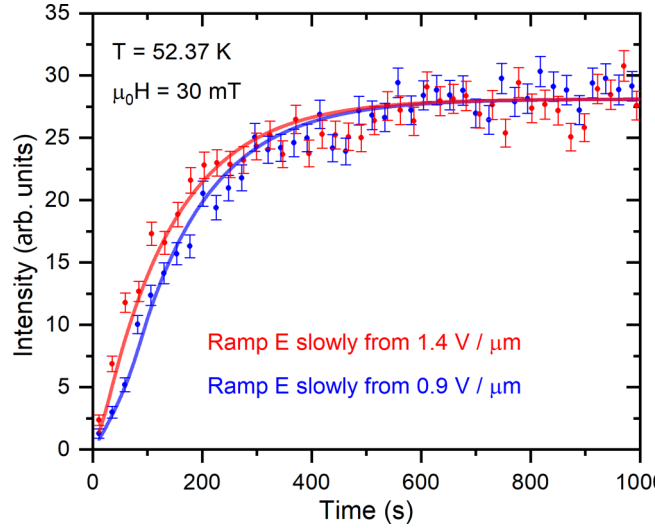

FIG. 8. Intensity of skyrmions as a function of time measured at $T = 52.25\,\mathrm{K}$ and $H = 30\,\mathrm{mT}$ for two different ramp rates of the electric field. Blue is for ramping fast to $0.9\,\mathrm{V}/\mu\mathrm{m}$ and $0.009\ (\mathrm{V}/\mu\mathrm{m})/\mathrm{s}$ up to $1.7\ \mathrm{V}/\mu\mathrm{m}$, while red is ramping fast to $1.4\,\mathrm{V}/\mu\mathrm{m}$ and $0.009\ (\mathrm{V}/\mu\mathrm{m})/\mathrm{s}$ up to $1.7\,\mathrm{V}/\mu\mathrm{m}$. Solid lines show fits to Eq. (A6) using parameters for the two different ramp rates. Both are fitted to the same formation time of $133 \pm 5\,\mathrm{s}$

electric field therefore requires a small correction to the fitting procedure to produce accurate formation times.

We first start with an exponential fitting function for the skyrmion intensity (S),

$$S = A\left(1 - e^{-\frac{t}{\tau}}\right), \tag{A1}$$

where A is a scale factor representing the final intensity at long times, t is the time, and τ is the formation time.

Next, assume τ varies linearly with time while the electric field changes, $\tau = a(1 + kt)$ for $t \leqslant t_0$, where t_0 is the end time of the electric field ramp, a is a scale factor, and k is the relative slope which we assume to be fixed as a function of magnetic field and temperature. Defining E_i as the electric field at the start of the slow ramp, and ϵ as the ramp rate, k can be determined from the fit in Fig. 7(b) as $k = \epsilon m/(b + mE_i) = 0.008\ \mathrm{s}^{-1}$ for $E_i = 0.9\,\mathrm{V}/\mu\mathrm{m}$ and $0.0133\ \mathrm{s}^{-1}$ for $E_i = 1.4\,\mathrm{V}/\mu\mathrm{m}$.

Now, writing $S(t) = A[1 - C(t)]$, the differential equation appropriate for an exponential process C is

$$dC/dt = -\frac{C}{\tau}. \tag{A2}$$

Allowing τ to depend on time as $\tau = a(1 + kt)$, this gives

$$dC/dt = -\frac{C}{a(1 + kt)}. \tag{A3}$$

Solving this equation yields

$$C = (1 + kt)^{\frac{-1}{ka}}. \tag{A4}$$

Hence, the skyrmion intensity for $t \leqslant t_0$ is given by

$$S = A\left[1 - (1 + kt)^{\frac{-1}{ka}}\right]. \tag{A5}$$

After t_0 the skyrmion intensity will be given by the exponential relationship [Eq. (A1)], scaled appropriately such that it is equal to Eq. (A5) at $t = t_0$. Therefore, the final expression for the skyrmion intensity at any time is

$$S = \begin{cases} A\left[1 - (1 + kt)^{\frac{-1}{ka}}\right], & \text{if} \quad t \leqslant t_0, \\ A\left[1 - e^{\frac{-t}{\tau}} \frac{(1+kt_0)^{\frac{-1}{ka}}}{e^{\frac{-t_0}{\tau}}}\right], & \text{if} \quad t > t_0. \end{cases} \tag{A6}$$

This equation allows data at different electric field ramp rates to be fitted with the same formation time (τ), as shown by Fig. 8. In the paper, the values we report as the formation time are the constant values τ takes for $t > t_0$, $\tau = a(1 + kt_0)$.

[1] F. D. M. Haldane, Nobel lecture: Topological quantum matter, Rev. Mod. Phys. **89**, 040502 (2017).

[2] M. Z. Hasan and C. L. Kane, Colloquium: Topological insulators, Rev. Mod. Phys. **82**, 3045 (2010).

[3] X.-L. Qi and S.-C. Zhang, Topological insulators and superconductors, Rev. Mod. Phys. **83**, 1057 (2011).

[4] N. Nagaosa and Y. Tokura, Topological properties and dynamics of magnetic skyrmions, Nat. Nanotechnol. **8**, 899 (2013).

[5] U. K. Rößler, A. N. Bogdanov, and C. Pfleiderer, Spontaneous skyrmion ground states in magnetic metals, Nature (London) **442**, 797 (2006).

[6] S. Mühlbauer, B. Binz, F. Jonietz, C. Pfleiderer, A. Rosch, A. Neubauer, R. Georgii, and P. Böni, Skyrmion lattice in a chiral magnet, Science **323**, 915 (2009).

[7] X. Z. Yu, N. Kanazawa, Y. Onose, K. Kimoto, W. Z. Zhang, S. Ishiwata, Y. Matsui, and Y. Tokura, Near room-temperature formation of a skyrmion crystal in thin-films of the helimagnet FeGe, Nat. Mater. **10**, 106 (2011).

[8] W. Münzer, A. Neubauer, T. Adams, S. Mühlbauer, C. Franz, F. Jonietz, R. Georgii, P. Böni, B. Pedersen, M. Schmidt, A. Rosch, and C. Pfleiderer, Skyrmion lattice in the doped semiconductor $Fe_{1-x}Co_xSi$, Phys. Rev. B **81**, 041203(R) (2010).

[9] S. Seki, X. Z. Yu, S. Ishiwata, and Y. Tokura, Observation of skyrmions in a multiferroic material, Science **336**, 198 (2012).

[10] Y. Tokunaga, X. Z. Yu, J. S. White, H. M. Rønnow, D. Morikawa, Y. Taguchi, and Y. Tokura, A new class of chiral materials hosting magnetic skyrmions beyond room temperature, Nat. Commun. **6**, 7638 (2015).

[11] Y. Fujima, N. Abe, Y. Tokunaga, and T. Arima, Thermodynamically stable skyrmion lattice at low temperatures in a bulk crystal of lacunar spinel GaV_4Se_8, Phys. Rev. B **95**, 180410(R) (2017).

[12] E. Ruff, S. Widmann, P. Lunkenheimer, V. Tsurkan, S. Bordács, I. Kézsmárki, and A. Loidl, Multiferroicity and skyrmions carrying electric polarization in GaV_4S_8, Sci. Adv. **1**, e1500916 (2015).

[13] S. Heinze, K. von Bergmann, M. Menzel, J. Brede, A. Kubetzka, R. Wiesendanger, G. Bihlmayer, and S. Blügel, Spontaneous atomic-scale magnetic skyrmion lattice in two dimensions, Nat. Phys. **7**, 713 (2011).

[14] C. Moreau-Luchaire, C. Moutafis, N. Reyren, J. Sampaio, C. A. F. Vaz, N. Van Horne, K. Bouzehouane, K. Garcia, C. Deranlot, P. Warnicke *et al.*, Additive interfacial chiral interaction in multilayers for stabilization of small individual skyrmions at room temperature, Nat. Nanotechnol. **11**, 444 (2016).

[15] A. Soumyanarayanan, M. Raju, A. L. Gonzalez Oyarce, A. K. C. Tan, M.-Y. Im, A. P. Petrović, P. Ho, K. H. Khoo, M. Tran, C. K. Gan *et al.*, Tunable room-temperature magnetic skyrmions in Ir/Fe/Co/Pt multilayers, Nat. Mater. **16**, 898 (2017).

[16] A. O. Leonov, Y. Togawa, T. L. Monchesky, A. N. Bogdanov, J. Kishine, Y. Kousaka, M. Miyagawa, T. Koyama, J. Akimitsu, Ts. Koyama *et al.*, Chiral Surface Twists and Skyrmion Stability in Nanolayers of Cubic Helimagnets, Phys. Rev. Lett. **117**, 087202 (2016).

[17] M. N. Wilson, A. B. Butenko, A. N. Bogdanov, and T. L. Monchesky, Chiral skyrmions in cubic helimagnet films: The role of uniaxial anisotropy, Phys. Rev. B **89**, 094411 (2014).

[18] F. N. Rybakov, A. B. Borisov, and A. N. Bogdanov, Three-dimensional skyrmion state in thin films of cubic helimagents, Phys. Rev. B **87**, 094424 (2013).

[19] T. Kurumaji, T. Nakajima, M. Hirschberger, A. Kikkawa, Y. Yamasaki, H. Sagayama, H. Nakao, Y. Taguchi, T. Arima, and Y. Tokura, Skyrmion lattice with a giant topological Hall effect in a frustrated triangular-lattice magnet, arXiv:1805.10719.

[20] M. Hirschberger, T. Nakajima, S. Gao, L. Peng, A. Kikkawa, T. Kurumaji, M. Kriener, Y. Yamasaki, H. Sagayama, H. Nakao *et al.*, Skyrmion phase and competing magnetic orders on a breathing kagome lattice, arXiv:1812.02553.

[21] A. Fert, V. Cros, and J. Sampaio, Skyrmions on the track, Nat. Nanotechnol. **8**, 152 (2013).

[22] A. Fert, N. Reyren, and V. Cros, Magnetic skyrmions: Advances in physics and potential applications, Nat. Rev. Mater. **2**, 17031 (2017).

[23] N. Romming, C. Hanneken, M. Menzel, J. E. Bickel, B. Wolter, K. von Bergmann, A. Kubetzka, and R. Wiesendanger, Writing and deleting single magnetic skyrmions, Science **341**, 636 (2013).

[24] A. J. Kruchkov, J. S. White, M. Bartkowiak, I. Živković, A. Magrez, and H. M. Rønnow, Direct electric field control of the skyrmion phase in a magnetoelectric insulator, Sci. Rep. **8**, 10466 (2018).

[25] J. S. White, I. Živković, A. J. Kruchkov, M. Bartkowiak, A. Magrez, and H. M. Rønnow, Electric-Field-Driven Topological Phase Switching and Skyrmion-Lattice Metastability in Magnetoelectric Cu_2OSeO_3, Phys. Rev. Appl. **10**, 014021 (2018).

[26] P. Huang, M. Cantoni, A. Kruchkov, J. Rajeswari, A. Magrez, F. Carbone, and H. M. Rønnow, In situ electric field skyrmion creation in magnetoelectric Cu_2OSeO_3, Nano Lett. **18**, 5167 (2018).

[27] Y. Okamura, F. Kagawa, S. Seki, and Y. Tokura, Transition to and from the skyrmion lattice phase by electric fields in a magnetoelectric compound, Nat. Commun. **7**, 12669 (2016).

[28] P. Milde, D. Köhler, J. Seidel, L. M. Eng, A. Bauer, A. Chacon, J. Kindervater, S. Mühlbauer, C. Pfleiderer, S. Buhrandt *et al.*, Unwinding of a skyrmion lattice by magnetic monopoles, Science **340**, 1076 (2013).

[29] H. Oike, A. Kikkawa, N. Kanazawa, Y. Taguchi, M. Kawasaki, Y. Tokura, and F. Kagawa, Interplay between topological and thermodynamic stability in a metastable magnetic skyrmion lattice, Nat. Phys. **12**, 62 (2016).

[30] K. Karube, J. S. White, N. Reynolds, J. L. Gavilano, H. Oike, A. Kikkawa, F. Kagawa, Y. Tokunaga, H. M. Rønnow, Y. Tokura, and Y. Taguchi, Robust metastable skyrmions and their triangular-square lattice structural transition in a high-temperature chiral magnet, Nat. Mater. **15**, 1237 (2016).

[31] A. Štefančič, S. H. Moody, T. J. Hicken, M. T. Birch, G. Balakrishnan, S. A. Barnett, M. Crisanti, J. S. O. Evans, S. J. R. Holt, K. J. A. Franke *et al.*, Origin of skyrmion lattice phase splitting in Zn-substituted Cu_2OSeO_3, Phys. Rev. Mater. **2**, 111402(R) (2018).

[32] M. T. Birch, R. Takagi, S. Seki, M. N. Wilson, F. Kagawa, A. Štefančič, G. Balakrishnan, R. Fan, P. Steadman, C. J. Ottley *et al.*, Increased lifetime of metastable skyrmions by doping, arXiv:1809.02590.

[33] M. Bartkowiak, J. S. White, H. M. Rønnow, and K. Prša, Note: Versatile sample stick for neutron scattering experiments in high electric fields, Rev. Sci. Instrum. **85**, 026112 (2014).

[34] P. Strunz, K. Mortensen, and S. Janssen, SANS-II at SINQ: Installation of the former Risø-SANS facility, Phys. B (Amsterdam) **350**, E783 (2004).

[35] C. D. Dewhurst, GRASP User Manual, Technical Report No. ILL03DE01T, Institut Laue-Langevin, Grenoble, 2003, http://www.ill.fr/lss/grasp.

[36] S. L. Zhang, A. Bauer, D. M. Burn, P. Milde, E. Neuber, L. M. Eng, H. Berger, C. Pfleiderer, G. van der Laan, and T. Hesjeda, Multidomain skyrmion lattice state in Cu_2OSeO_3, Nano Lett. **16**, 3285 (2016).

[37] K. Makino, J. D. Reim, D. Higashi, D. Okuyama, T. J. Sato, Y. Nambu, E. P. Gilbert, N. Booth, S. Seki, and Y. Tokura, Thermal stability and irreversibility of skyrmion-lattice phases in Cu_2OSeO_3, Phys. Rev. B **95**, 134412 (2017).

[38] J. S. White, I. Levatić, A. A. Omrani, N. Egetenmeyer, K. Prša, I. Živković, J. L. Gavilano, J. Kohlbrecher, M. Bartkowiak, H. Berger, and H. M. Rønnow, Electric field control of the skyrmion lattice in Cu_2OSeO_3, J. Phys.: Condens. Matter **24**, 432201 (2012).

[39] C. Dhital, L. DeBeer-Schmitt, D. P. Young, and J. F. DiTusa, Unpinning the skyrmion lattice in MnSi: Effect of substitutional disorder, Phys. Rev. B **99**, 024428 (2019).

[40] T. Reimann, A. Bauer, C. Pfleiderer, P. Böni, P. Trtik, A. Tremsin, M. Schulz, and S. Mühlbauer, Neutron diffraction imaging of the skyrmion lattice nucleation in MnSi, Phys. Rev. B **97**, 020406(R) (2018).

[41] J. Wild, T. N. G. Meier, S. Pöllath, M. Kronseder, A. Bauer, A. Chacon, M. Halder, M. Schowalter, A. Rosenauer, J. Zweck *et al.*, Entropy-limited topological protection of skyrmions, Sci. Adv. **3**, e1701704 (2017).

[42] L. Peng, Y. Zhang, L. Ke, T.-H. Kim, Q. Zheng, J. Yan, X.-G. Zhang, Y. Gao, S. Wang, J. Cai *et al.*, Relaxation dynamics of zero-field skyrmions over a wide temperature range, Nano Lett. **18**, 7777 (2018).

[43] F. Büttner, I. Lemesh, and G. S. D. Beach, Theory of isolated magnetic skyrmions: From fundamentals to room temperature applications, Sci. Rep. **8**, 4464 (2018).

[44] J. Sampaio, V. Cros, S. Rohart, A. Thiaville, and A. Fert, Nucleation, stability and current-induced motion of isolated magnetic skyrmions in nanostructures, Nat. Nanotechnol. **8**, 839 (2013).

[45] F. Kagawa, H. Oike, W. Koshibae, A. Kikkawa, Y. Okamura, Y. Taguchi, N. Nagaosa, and Y. Tokura, Current-induced viscoelastic topological unwinding of metastable skyrmion strings, Nat. Commun. **8**, 1332 (2017).

[46] J. Romhányi, J. van den Brink, and I. Rousochatzakis, Entangled tetrahedron ground state and excitations of the magnetoelectric skyrmion material Cu_2OSeO_3, Phys. Rev. B **90**, 140404(R) (2014).

[47] K. J. A. Franke, P. R. Dean, M. C. Hatnean, M. T. Birch, D. Khalyavin, P. Manuel, T. Lancaster, G. Balakrishnan, and P. D. Hatton, Investigating the magnetic ground state of the skyrmion host material Cu_2OSeO_3 using long-wavelength neutron diffraction, arXiv:1807.11333.

[48] G. S. Tucker, J. S. White, J. Romhányi, D. Szaller, I. Kézsmárki, B. Roessli, U. Stuhr, A. Magrez, F. Groitl, P. Babkevich *et al.*, Spin excitations in the skyrmion host Cu_2OSeO_3, Phys. Rev. B **93**, 054401 (2016).

[49] http://dx.doi.org/10.15128/r26395w7101.